



ORNL/TM-1999/133

**OAK RIDGE  
NATIONAL  
LABORATORY**

LOCKHEED MARTIN



**Thermal and Physical  
Property Determinations  
for Ionsiv<sup>®</sup> IE-911  
Crystalline Silicotitanate  
and Savannah River Site  
Waste Simulant Solutions**

D. T. Bostick  
W. V. Steele

MANAGED AND OPERATED BY  
LOCKHEED MARTIN ENERGY RESEARCH CORPORATION  
FOR THE UNITED STATES  
DEPARTMENT OF ENERGY

ORNL-27 (3-96)



Chemical Technology Division

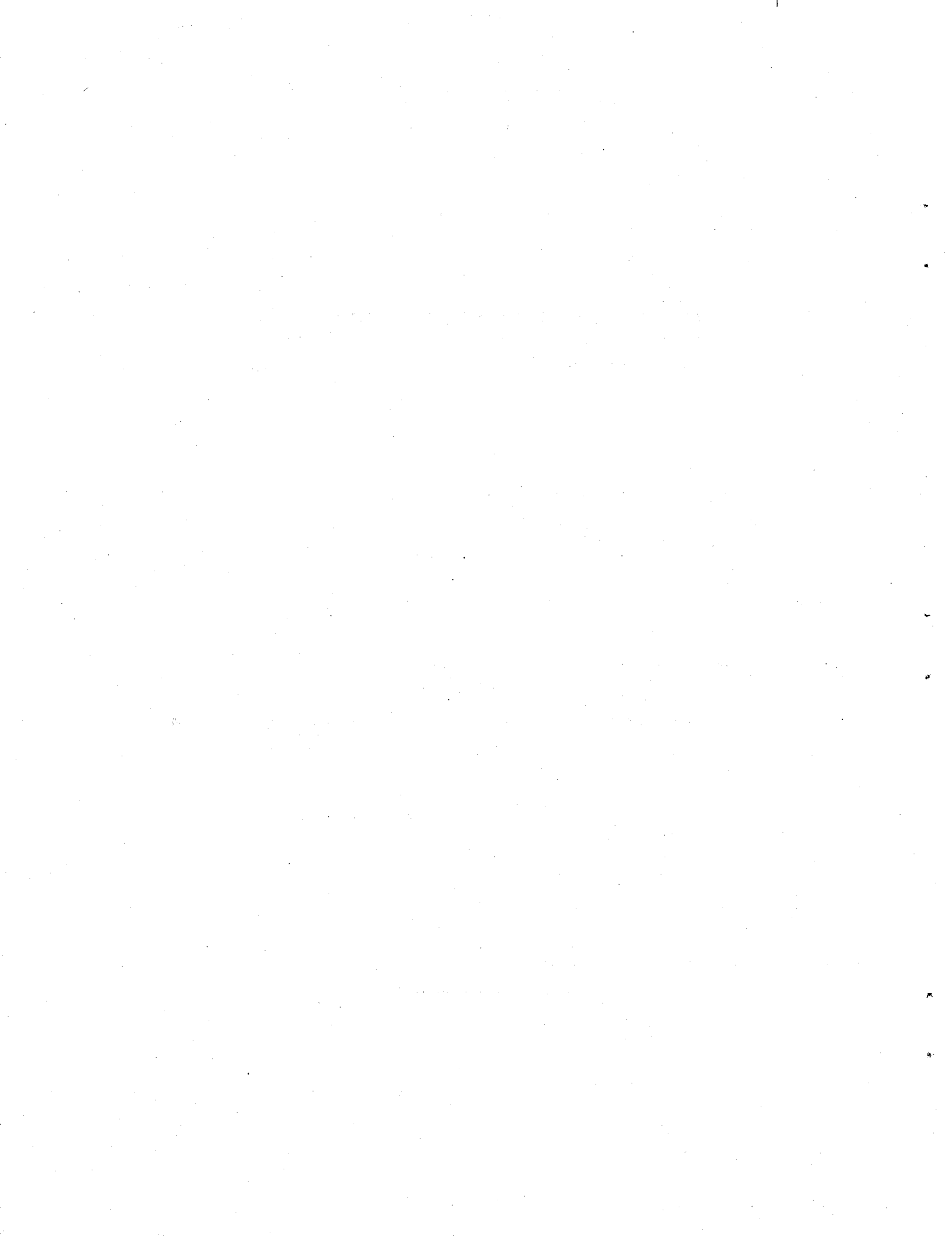
**Thermal and Physical Property Determinations for  
Ionsiv<sup>®</sup> IE-911 Crystalline Silicotitanate and  
Savannah River Site Waste Simulant Solutions**

D. T. Bostick and W. V. Steele

Date Published – August 1999

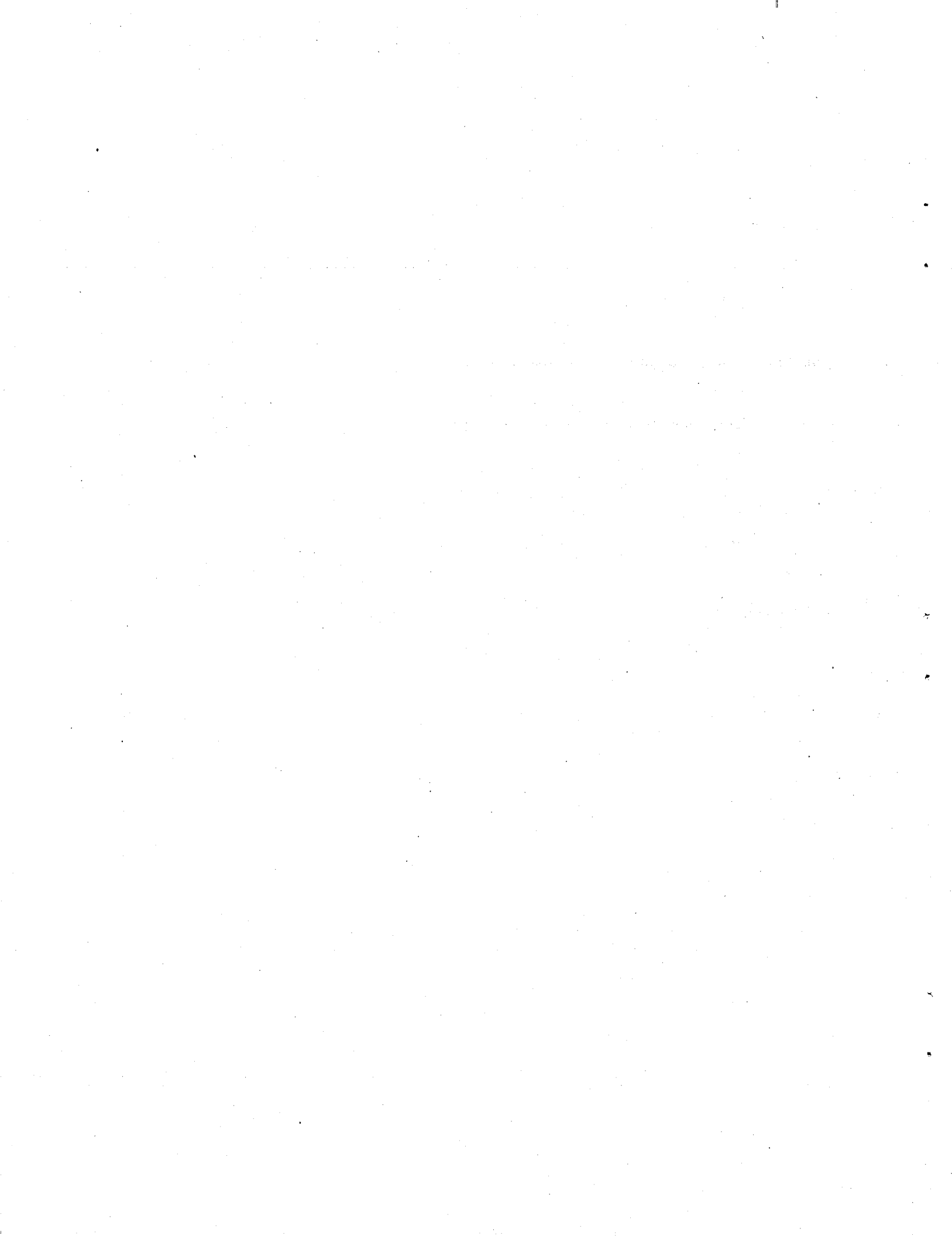
Prepared for the  
U.S. Department of Energy Office of Science and Technology  
Tank Focus Area

Prepared by the  
OAK RIDGE NATIONAL LABORATORY  
Oak Ridge, Tennessee 37831-6285  
managed by  
LOCKHEED MARTIN ENERGY RESEARCH CORP.  
for the  
U.S. DEPARTMENT OF ENERGY  
under contract DE-AC05-96OR22464



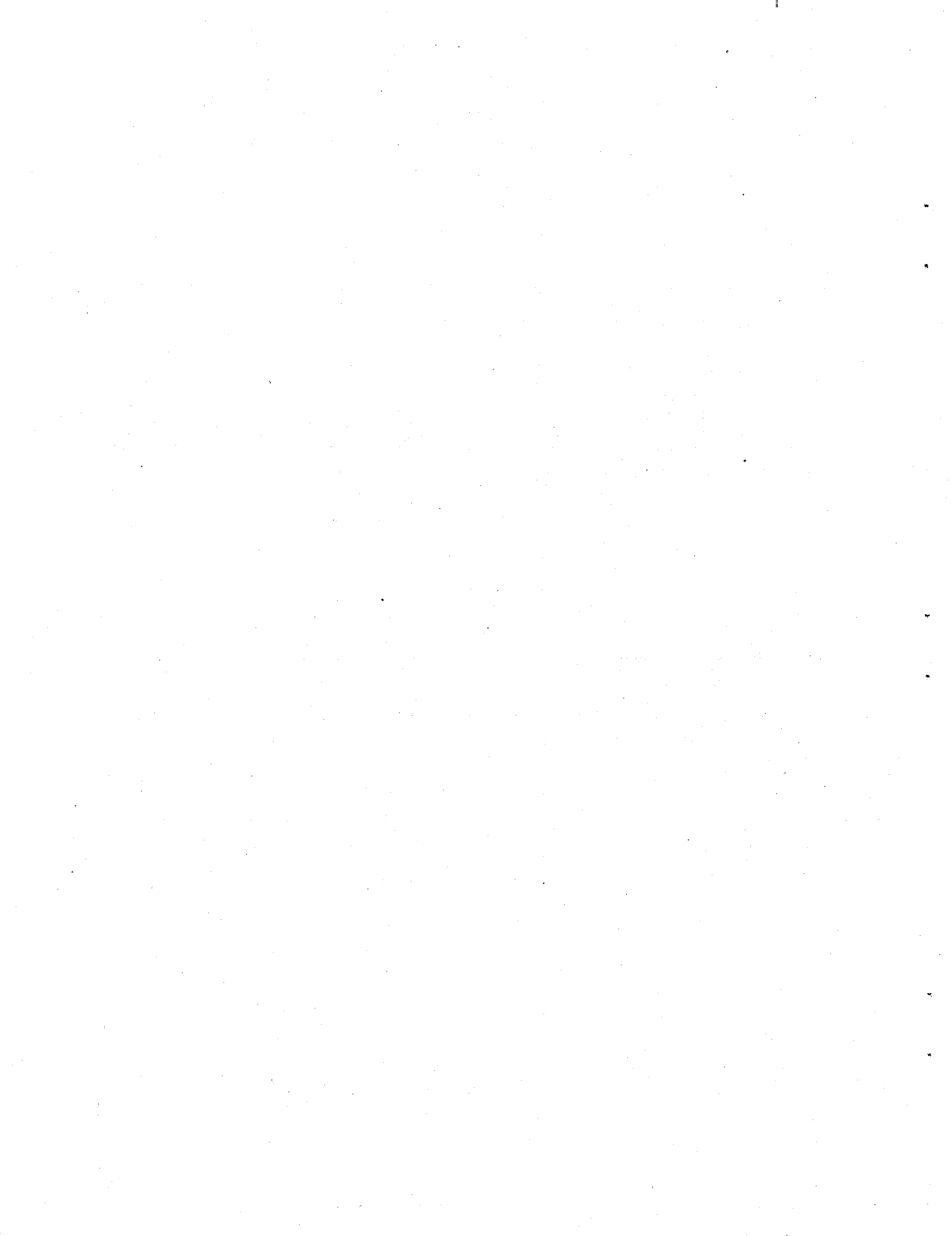
## CONTENTS

LIST OF TABLES .....	v
LIST OF FIGURES .....	vii
ABSTRACT .....	ix
1. INTRODUCTION .....	1
1.1 SCOPE OF WORK .....	1
1.2 DESCRIPTION OF TASK .....	1
1.3 DESIGNATION OF IONSIV® IE-911 SAMPLES .....	3
2. PHYSICAL PROPERTIES OF IONSIV® IE-911 .....	3
2.1 SIEVE ANALYSIS .....	3
2.2 SURFACE MOISTURE CONTENT .....	6
2.3 SORBENT POROSITY AND SURFACE AREA .....	6
3. THERMOPHYSICAL PROPERTIES OF IONSIV® IE-911 .....	9
3.1 DSC METHODOLOGY .....	9
3.2 PURE CRYSTALLINE SILICOTITANATE .....	10
3.3 AS-RECEIVED IONSIV® IE-911 SAMPLES .....	12
3.4 PRETREATED IONSIV® IE-911 SAMPLES .....	12
3.5 PRECURSOR TO BINDER AND CST BINDER .....	14
4. THERMOPHYSICAL PROPERTIES OF SRS WASTE SIMULANTS .....	17
4.1 PREPARATION OF WASTE SIMULANTS .....	17
4.2 DETERMINATION OF SOLUTION DENSITY .....	19
4.3 FORMATION OF SOLIDS AT LOW TEMPERATURE .....	21
4.4 DETERMINATION OF SIMULANT VISCOSITY .....	22
4.5 DETERMINATION OF HEAT CAPACITY .....	23
4.6 DETERMINATION OF THERMAL CONDUCTIVITY .....	24
5. SUMMARY .....	27
6. REFERENCES .....	29



## LIST OF TABLES

Table		Page
1	Composition of SRS waste simulants .....	2
2	Weight distribution of as-received Ionsiv® IE-911, lot 999098810005 .....	4
3	Overall sieve analysis results for Ionsiv® IE-911 lot 999098810005 .....	5
4	Water content of Ionsiv® IE-911, lot 999098810005 .....	6
5	BET surface area and porosity of Ionsiv® IE-911, lot 999098810005 .....	9
6	Samples studied in DSC analyses .....	10
7	Densities of SRS simulants determined on a weight basis .....	17
8	Regression equations for the determination of SRS simulant densities .....	19
9	Calculated densities of SRS simulants .....	21
10	Viscosities of SRS simulants .....	22
11	Determination of heat capacities for SRS simulants .....	23
12	Results of experimental thermal conductivity (W/m·K) measurements for SRS simulants .....	24
13	Calculated thermal conductivity values for SRS simulants .....	26



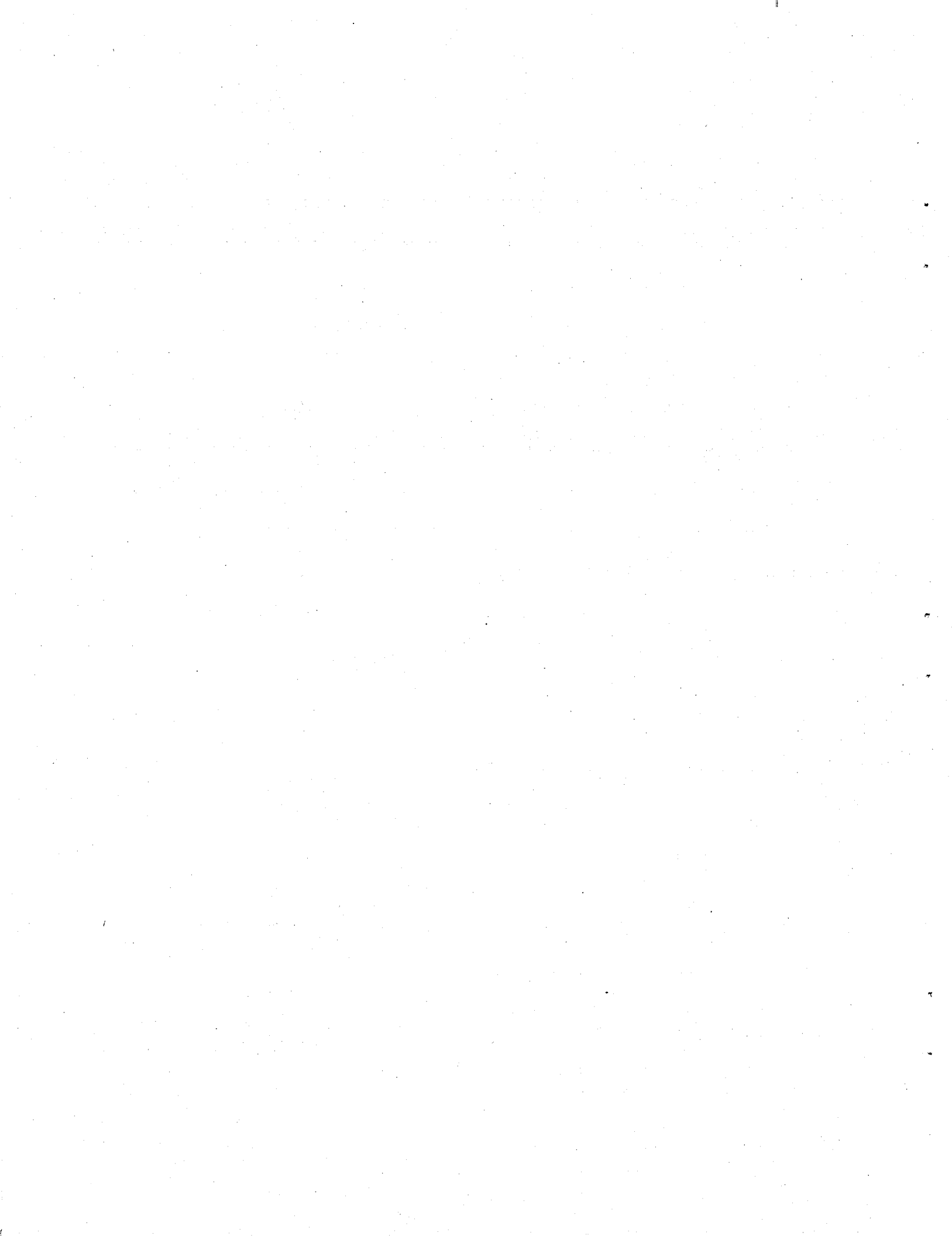
## LIST OF FIGURES

Figure		Page
1	BET nitrogen sorption profile of as-received Ionsiv <sup>®</sup> IE-911 .....	7
2	DSC scan of pure CST powder (Ionsiv <sup>®</sup> IE-910) .....	11
3	DSC scan of as-received Ionsiv <sup>®</sup> IE-911, lot 999098810005 .....	13
4	DSC scan of pretreated Ionsiv <sup>®</sup> IE-911, lot 999098810005 .....	15
5	DSC scan of precursor to CST binder .....	16
6	DSC scan of CST binder in Ionsiv <sup>®</sup> IE-911 .....	18
7	Experimental versus literature values for densities of NaCl standards .....	20
8	Variation of simulant density with temperature .....	20



## ABSTRACT

This document describes physical and thermophysical property determinations that were made in order to resolve questions associated with the decontamination of Savannah River Site (SRS) waste streams using ion exchange on crystalline silicotitanate (CST). The research will aid in the understanding of potential issues associated with cooling of feed streams within SRS waste treatment processes. Toward this end, the thermophysical properties of engineered CST, manufactured under the trade name, Ionsiv® IE-911 by UOP, Mobile, AL, were determined. The heating profiles of CST samples from several manufacturers' production runs were observed using differential scanning calorimetric (DSC) measurements. DSC data were obtained over the region of 10 to 215°C to check for the possibility of a phase transition or any other enthalpic event in that temperature region. Finally, the heat capacity, thermal conductivity, density, viscosity, and salting-out point were determined for SRS waste simulants designated as "Average," "High NO<sub>3</sub><sup>-</sup>," and "High OH<sup>-</sup>" simulants.



## 1. INTRODUCTION

### 1.1 SCOPE OF WORK

This document describes physical and thermophysical property determinations that were made in order to resolve questions associated with the decontamination of Savannah River Site (SRS) waste streams using ion exchange on crystalline silicotitanate (CST). The scope of work was requested by SRS<sup>1</sup> and performed according to the ORNL Task Plan ORNL/CF-99/4.<sup>2</sup> The research will aid in the understanding of potential issues associated with the cooling of feed streams within SRS waste treatment processes. To this end, the thermophysical properties of engineered CST sorbent (manufactured under the product name Ionsiv<sup>®</sup> IE-911 by UOP, Mobile, Alabama) were measured to provide information so that a total heat balance could be completed for large-scale CST columns. Ancillary to this task, the stability of CST in the temperature region ambient to 215°C was addressed to determine whether Ionsiv<sup>®</sup> IE-911 undergoes a solid-phase transition in the region of 80°C. Finally, the heat capacity, thermal conductivity, density, viscosity, and salting-out point were determined for SRS waste simulants designated as "Average," "High NO<sub>3</sub><sup>-</sup>," and "High OH<sup>-</sup>" simulants.

### 1.2 DESCRIPTION OF TASK

This task consisted of the following activities:

1. Subjection of CST samples to differential scanning calorimetric measurements in the region of 25 to 215°C to check for the possibility of a phase transition or any other enthalpic event in that temperature region.
2. Measurement of the porosities of samples of CST.

3. Determination of physical properties of the SRS waste simulants designated as "Average," "High NO<sub>3</sub><sup>-</sup>," or "High OH<sup>-</sup>" (see Table 1).<sup>3</sup> The physical properties to be measured were heat capacity and thermal conductivity at 30°C, density at 10 and 30°C, and viscosity at 10 and 30°C.
4. Determination of the salting-out point for each SRS waste simulant.

The experimental details for each determination are given in the respective sections of this report.

**Table 1. Composition of SRS waste simulants<sup>a</sup>**

Component	Simulant concentration (M)		
	Average	High OH <sup>-</sup>	High NO <sub>3</sub> <sup>-</sup>
<b>Anion</b>			
OH <sup>-</sup>	1.91	3.05	1.17
NO <sub>3</sub> <sup>-</sup>	2.14	1.08	2.84
NO <sub>2</sub> <sup>-</sup>	0.52	0.74	0.37
Cl <sup>-</sup>	0.025	0.010	0.040
CO <sub>3</sub> <sup>2-</sup>	0.16	0.17	0.16
PO <sub>4</sub> <sup>3-</sup>	0.01	0.008	0.01
C <sub>2</sub> O <sub>4</sub> <sup>2-</sup>	0.008	0.008	0.008
F <sup>-</sup>	0.032	0.01	0.05
SiO <sub>3</sub> <sup>2-</sup>	0.004	0.004	0.004
MoO <sub>4</sub> <sup>2-</sup>	0.0002	0.0002	0.0002
AlO <sub>2</sub> <sup>-</sup>	0.31	0.27	0.32
SO <sub>4</sub> <sup>2-</sup>	0.15	0.03	0.22
<b>Cation</b>			
Na <sup>+</sup>	5.6	5.6	5.6
K <sup>+</sup>	0.015	0.03	0.0041
Cs <sup>+</sup>	0.00014	0.00037	0.00014

<sup>a</sup>D. D. Walker, *Preparation of Simulated Waste Solutions*, WSRC-TR-99-00116, April 15, 1999.

### 1.3 DESIGNATION OF IONSIV® IE-911 SAMPLES

Several production runs were made by UOP during the development of Ionsiv® IE-911 for commercial distribution. The engineered CST prepared in the 1996 campaign was designated with a lot number (having the sequence 99909681000x, where  $x = 1, 2, 3, 4$ ); portions of the various lots have been archived at ORNL. A sample of the pure CST powder, without binder, has also been archived and has the lot number 993796040005. More recently, eight additional lots were prepared in a 1998 production run and delivered to Oak Ridge National Laboratory (ORNL) in January 1999. The new material received after batch 4 (from the old numbering system) has lot numbers 99909881000x, where  $x = 1$  through 8 (two 55-gal drums per lot) for a total of 16 drums of Ionsiv® IE-911. A final sample of engineered CST (lot 999099810009) was received in June 1999. In our studies of solid-phase transition, archived samples of engineered and powdered CST were compared with the recently received Ionsiv® IE-911 to help interpret differential scanning calorimetric profiles.

## 2. PHYSICAL PROPERTIES OF IONSIV® IE-911

### 2.1 SIEVE ANALYSIS

Samples of Ionsiv® IE-911, lot 99909881005, were tested using both dry- and wet-sieving techniques. Approximately 30 g of sorbent was selected from the lot through multiple passes of 250 g of sorbent through a riffle splitter. The 30-g sample was placed in the top of a series of sieve pans spanning the range of 20–100 mesh (149–840  $\mu\text{m}$ ); a solid pan was placed at the bottom of the sieves to collect the sorbent fines. For dry-sieve testing, the stack of sieves was shaken for 20 min on a W. S. Tyler Model RX24 sieve shaker. The contents of each sieve were weighed to determine the weight percent of sorbent collected in each size range. Typical sieving results are presented in Table 2. The standard deviation in

mesh size was based on using the weight percent CST for a particle size representing the mid-point diameter ( in units of  $\mu\text{m}$ ) for a given sieve pan.

**Table 2. Weight distribution of as-received Ionsiv® IE-911, lot 999098810005**

U.S. sieve	Particle size ( $\mu\text{m}$ )	Net weight (g)	% Total weight
30	<840/>590	2.15	6.22
35	<590/>500	6.39	18.47
40	<500/>420	10.55	30.48
50	<420/>297	15.84	45.80
60	<297/>250	0.43	1.24
100	<250/>149	0.02	0.06
>100	<149	0.03	0.08
Sum		35.4	102.3
Avg. mesh size:		443 $\mu\text{m}$	
Standard deviation of mesh size:		76 $\mu\text{m}$	

The wet-particle size was determined by first soaking 30-g samples, in triplicate, in deionized water for 24 h. Then, water was flowed through the stack of sieves for up to 2 h to complete sorbent sizing. The contents of the sieve pans were air-dried prior to weighing the CST.

As can be seen in Table 3, the dry- and wet-particle sizes for as-received CST were  $410 \pm 10 \mu\text{m}$  and  $440 \pm 10 \mu\text{m}$ , respectively. The stated standard deviation in Table 3 represents variation in the average mesh size calculated for each of the three sieve tests for the as-received Ionsiv® IE-911.

Sieve testing was also performed on pretreated Ionsiv® IE-911. The as-received CST was converted to the sodium form according to vendor instructions. Water was recirculated through ten-gal batches of as-received Ionsiv® IE-911. Fifty weight-percent NaOH was slowly added to the water until the pH of the

recirculating stream was in the 12.5-13 pH range. A total of 9 kg 50% NaOH was added in each CST conversion batch, giving a final NaOH concentration of 12 g/L (0.3 M NaOH) in the recirculating stream. Tap water was then flowed up through the sodium-form CST at a rate of 3 gpm, which expanded the CST bed volume by about 15%. The converted CST was rinsed until the column effluent was clear, which typically required 1 hour (~18 bed volumes water.)

Sieve results indicate that the dry- and wet-particle sizes of the pretreated CST are  $410 \pm 10 \mu\text{m}$  and  $460 \pm 20 \mu\text{m}$ , respectively. Greater than 95 wt % of each form of the sorbent was in the 30–50 mesh range ( $<-590/>250 \mu\text{m}$ ). Less than 1 wt % fines were collected in any sieve test of the sorbent. This is in contrast to archived Ionsiv® IE-911 lots, which typically contained up to 10% fines. The percent swelling stated in Table 3 was based on the relative sizes of the dry- and wet-sieve results for each CST source. In comparison, earlier sieve testing with lot 99909680002 data determined that particle size increased by approximately 20% when CST was soaked overnight in water.<sup>4</sup>

**Table 3 . Overall sieve analysis results for Ionsiv® IE-911  
Lot 999098810005**

CST source	Type of sieve	Average particle size ( $\mu\text{m}$ )	Standard deviation in 3 trials ( $\mu\text{m}$ )	% swelling
As-received	Dry	410	9	6.6
	Wet	437	12	
Pretreated	Dry	412	8	10.9
	Wet	457	18	

## 2.2 SURFACE MOISTURE CONTENT

The percent moisture was determined by heating 1-g samples of as-received and pretreated Ionsiv® IE-911 (lot 999098810005), in triplicate at 102–106 °C until a constant dry weight was achieved. CST samples were cooled in a desiccator prior weight determination. The moisture content of each form of CST was  $6.9 \pm 0.04$  %. Experimental results are given in Table 4.

Table 4. Water content of Ionsiv® IE-911,  
lot 999098810005

	As received (%)	Pretreated (%)
Trial 1	6.924	6.975
Trial 2	6.929	6.919
Trial 3	6.919	6.879
Average	6.924	6.915
Standard deviation	0.004	0.042

## 2.3 SORBENT POROSITY AND SURFACE AREA

The surface area and pore volume of as-received and prepared Ionsiv® IE-911 were determined using a Micromeritics Gemini 2375 system. The instrumentation can provide nitrogen sorption data for relative nitrogen pressures above 0.01. As such, the surface area and pore volume of CST, but not pore diameter range, can be measured reproducibly with this equipment. A 40-point nitrogen adsorption pressure profile was developed for each sample; each point had an equilibration time of 2 min. Most of the physisorption isotherms were typically grouped into six classes;<sup>1</sup> the isotherms of both as-received and pretreated Ionsiv® IE-911 correspond to Type II sorption behavior (Fig. 1). The reversible Type II isotherm is the normal form of isotherm obtained with a nonporous or macroporous adsorbent. The Type II isotherm represents unrestricted monolayer-multilayer adsorption. The beginning of the almost linear middle section of the

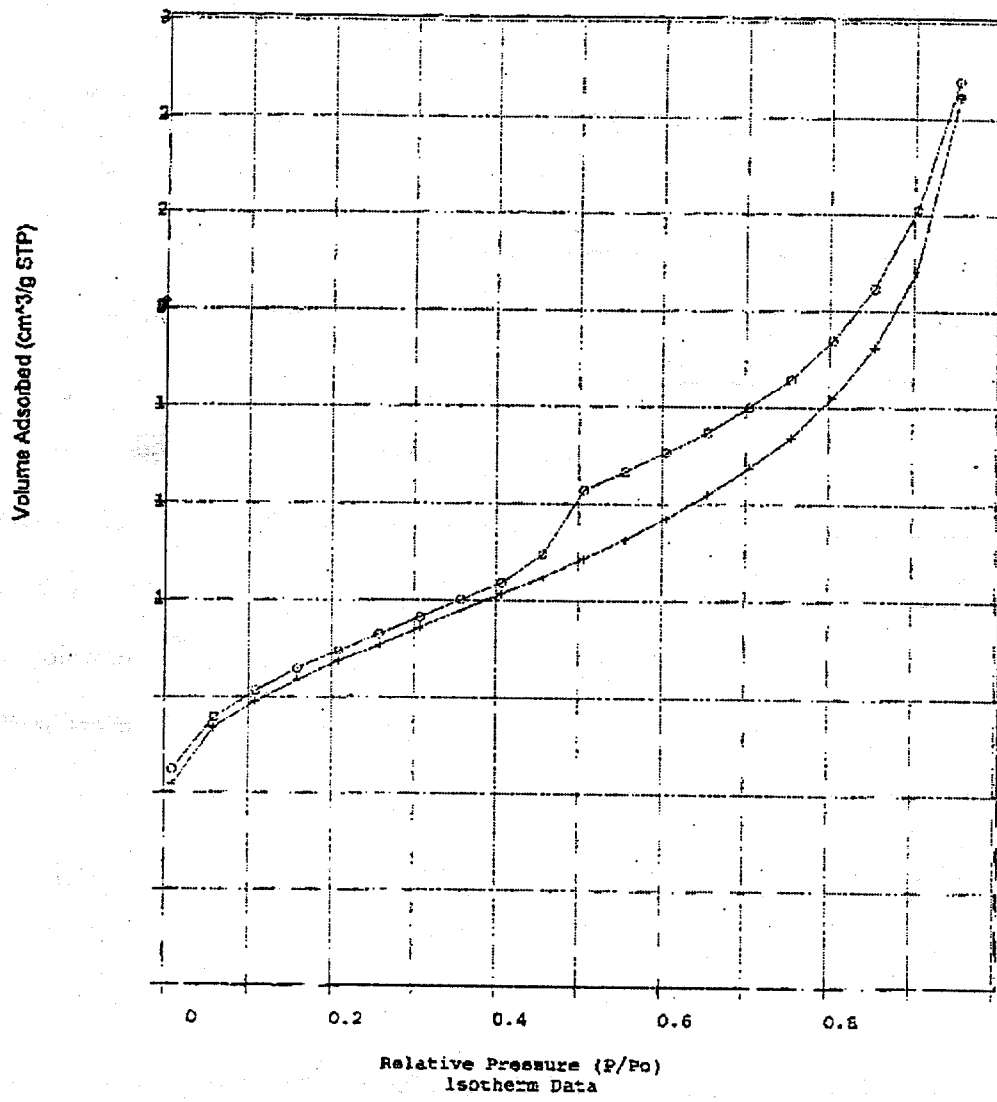


Fig. 1. BET nitrogen sorption profile of pretreated Ionsiv® IE-911.

isotherm is often taken to indicate the stage at which monolayer coverage is complete and multilayer adsorption begins.

Both types of Ionsiv<sup>®</sup> IE-911 samples exhibited a corresponding hysteresis between profiles obtained when the nitrogen pressure was either increased or decreased to obtain Brunauer, Emmett, and Teller (BET) isotherm results. Hysteresis appearing in the multilayer range of physisorption isotherms is usually associated with capillary condensation in mesopore structures. Such hysteresis loops may exhibit a wide variety of shapes, usually grouped into four main classifications (H1–H4). Although the effects of various factors on adsorption hysteresis are not fully understood, the shapes of hysteresis loops have often been identified with specific pore structures.<sup>5</sup> The CST isotherms are indicative of type H3 hysteresis, which does not exhibit any limiting adsorption at high nitrogen  $p/p_0$ . H3 hysteresis is observed in sorbents having with aggregates of plate-like particles, giving rise to slit-shaped pores. Early characterization work on CST powder confirms this finding. Dosch et al.<sup>6,7,8</sup> found that CST is comprised of layers of silicotitanate crystal; spacing between the crystals can be controlled such that the larger cesium ions can be sandwiched between the crystalline layer, whereas the smaller sodium ions can move freely throughout the crystal structure.

Table 5 summarizes the primary results obtained for 1-g samples of as-received and pretreated CST, analyzed in triplicate. BET scans were performed after the samples had been heated at 60°C for several days to remove surface moisture from the CST. It is clear that both surface area and pore volume were reduced after CST treatment with NaOH. This implies that some adsorption sites were occupied by adsorbates during pretreatment.

Table 5. BET surface area and porosity of Ionsiv® IE-911,  
lot 99909881005

Type of Material	Surface area (m <sup>2</sup> /g)	Micropore volume (cm <sup>3</sup> /g)	Total pore volume (cm <sup>3</sup> /g)
As-received	51	0.011	0.063
As-received	50	0.0098	0.063
As-received	51	0.010	0.063
Pretreated	35	0.0052	0.044
Pretreated	34	0.0053	0.043
Pretreated	31	0.0036	0.049

### 3. THERMOPHYSICAL PROPERTIES OF IONSIV® IE-911

#### 3.1 DSC METHODOLOGY

The use of a differential scanning calorimeter (DSC) in the determination of phase transitions and compound stabilities over a range of temperatures is well documented in the literature.<sup>9</sup> A Perkin-Elmer DSC 7 instrument in conjunction with the manufacturer's Pyris software package (Windows NT Pyris, Version 2) was used in the study reported here. Measurements were made using the heat-equilibration-heat step method detailed by Mraw and Naas<sup>10</sup>. The CST samples were confined in high-pressure cells fabricated from 17-4 PH chromium-nickel stainless steel (AISI No. 630)<sup>9</sup>. Each cell, with an internal volume of ~50  $\mu$ L, was sealed using a gold gasket made in the form of a washer. Initially, studies were made with 20°C cycles, heating at 5°C/min with a 2-min equilibration period between successive heats. Later, studies were made with 40°C cycles, heating at 5°C/min with a 4-min equilibration period between successive heats. Samples were studied over the temperature range 35–215°C. Sapphire [NIST Reference Standard Material (SRM720)] was used as the calibrant of both the enthalpy and the heat capacity scales of the DSC<sup>11</sup>. The temperature scale of the DSC was calibrated by the determination of the melting point of NIST Standard Reference Material indium. All DSC measurements were made in duplicate. Each

sample was sealed in the DSC cell under an ambient air atmosphere. Table 6 summarizes the CST (pure and engineered) samples studied in the DSC.

Table 6. Samples studied in DSC analyses

Lot	Type of sample	Type of Ionsiv <sup>®</sup>
993796040005	As-received	Ionsiv <sup>®</sup> IE-910 (pure CST)
999096810001	As-received	Ionsiv <sup>®</sup> IE-911
999096810002	As-received	Ionsiv <sup>®</sup> IE-911
999096810004	As-received	Ionsiv <sup>®</sup> IE-911
999098810005	As-received	Ionsiv <sup>®</sup> IE-911
999098810008	As-received	Ionsiv <sup>®</sup> IE-911
999098810005	Pretreated	Ionsiv <sup>®</sup> IE-911
999098810007	Pretreated	Ionsiv <sup>®</sup> IE-911
999098810008	Pretreated	Ionsiv <sup>®</sup> IE-911

### 3.2 PURE CRYSTALLINE SILICOTITANATE

DSC measurements of a sample of the pure CST powder without binder (Ionsiv<sup>®</sup> IE-910, lot 993796040005) were made as a reference for the study of the Ionsiv<sup>®</sup> IE-911 samples. The heat capacity of this sample varied linearly with temperature over the range of 35–215°C (Fig. 2) and can be represented by the following equation:

$$\text{Heat capacity (J} \cdot \text{g}^{-1} \cdot \text{°C}^{-1}\text{)} = 0.003676 T(\text{°C}) + 0.871, T = 35\text{--}215\text{°C} \quad (1)$$

Heat capacity values were reproducible to within  $\pm 1\%$  for duplicate measurements.

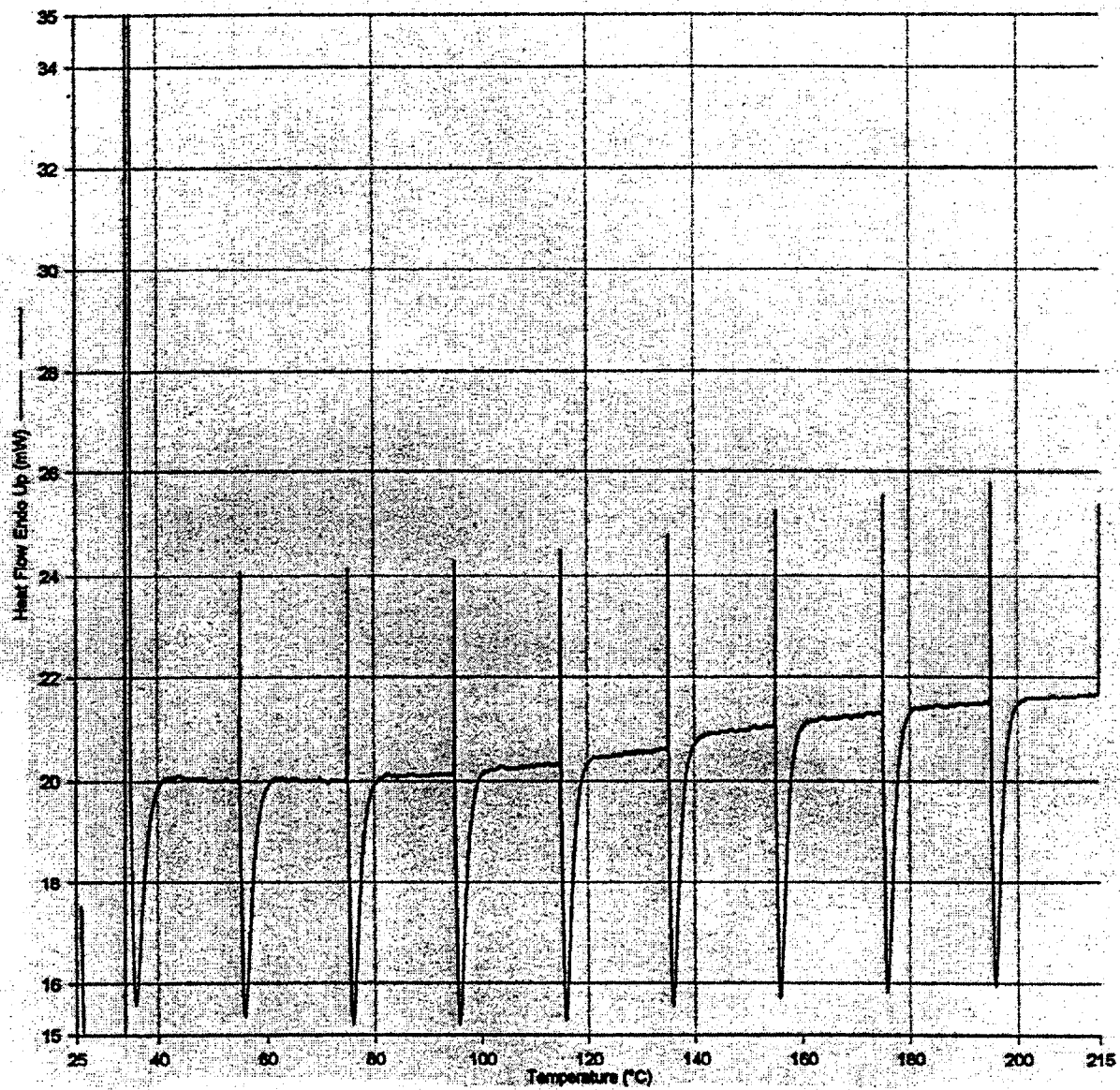


Fig. 2. DSC scan of pure CST powder (Ionsiv® IE-910).

An anomaly may exist in the heat capacity centered at 100°C with an enthalpy of 0.4 J·g<sup>-1</sup>; however, further studies would be required to verify its existence. The samples of pure CST studied showed no signs of charring or color change as the result of being heated to 215°C.

### 3.3 AS-RECEIVED IONSIV® IE-911 SAMPLES

Results of studies using Ionsiv® IE-911 samples from lots 999096810001 and 999096810004 indicated the presence of small exothermic heats centered at 175°C superimposed on a basic heat capacity-versus-temperature profile (Fig. 3) represented by Eq. (1).

DSC scans of Ionsiv® IE-911 samples from lots 999098810005 and 999098810008 showed evidence of what was initially interpreted as an endothermic reaction followed by an exothermic reaction. The centers of the reaction peaks shifted with the sample studied but appeared in the temperature range 105–165°C. Closer scrutiny of the equilibration cycles between the heats (see above) revealed that true equilibration was never reached. By increasing sample temperature continuously, rather than using heating cycles, it became apparent the correct interpretation of the DSC traces was the presence of an endothermic reaction spread across the temperature region 105°C–185°C. In addition to the endothermic reaction, the samples showed “graying” of most of the particles and even some charring that had occurred during the heating period in the DSC. The size of the peak for the samples from lot 999098810005 was larger than that for lot 999098810008; however, no attempt was made to quantify this difference.

### 3.4 PRETREATED IONSIV IE-911 SAMPLES

Samples of Ionsiv® IE-911 pretreated in accordance with the manufacturer’s instructions were also analyzed in the DSC. The lot numbers of the samples included in the analysis were 999098810005,

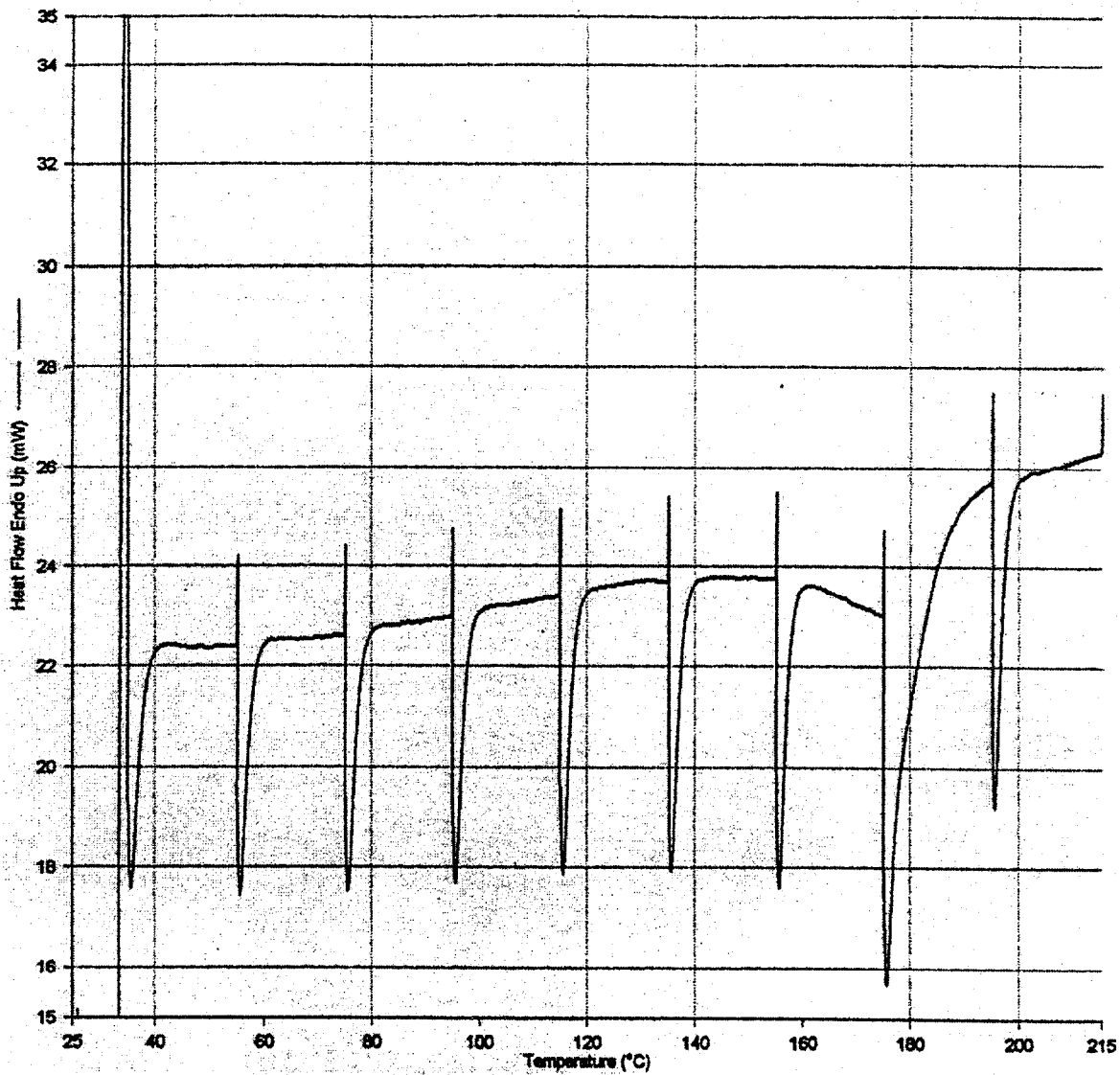


Fig. 3. DSC scan of as-received Ionsiv® IE-911, lot 0999098810005.

999098810007, and 999098810008. The derived heat capacities for the profile in Fig. 4 can be represented by the equations

$$\text{Heat capacity (J} \cdot \text{g}^{-1} \cdot \text{°C}^{-1}\text{)} = 0.00289T (\text{°C}) + -.98, T = 35\text{--}130\text{°C} \quad (2)$$

and

$$\text{Heat capacity (J} \cdot \text{g}^{-1} \cdot \text{°C}^{-1}\text{)} = 0.00489 T(\text{°C}) + 0.75, T = 130\text{--}215\text{°C} \quad (3)$$

Again, heat capacity values for both portions of the profile were reproducible to within  $\pm 1\%$  for duplicate measurements.

No registered heat was associated with the change in temperature dependence of sample heat capacity in the region of 130°C. Also, none of the “pretreated” samples showed evidence of graying or charring during the heating period in the DSC.

### 3.5 PRECURSOR TO THE BINDER AND CST BINDER

Following discussions with UOP, a laboratory chemical representing the precursor to the binder in Ionsiv® IE-911, Trade Secret 2 (TS2), was studied in the DSC. Like the majority of the recent “as-received” engineered Ionsiv® IE-911 samples studied, TS2 showed a wide endothermic reaction peak spread between 105 and 185°C (Fig. 5). The DSC trace showed the possibility that several reactions were superimposed on each other. In addition, the further “reaction” shown above 185°C prevented any meaningful calculation of the total heat of reaction in the 105–185°C region. No charring or graying occurred.

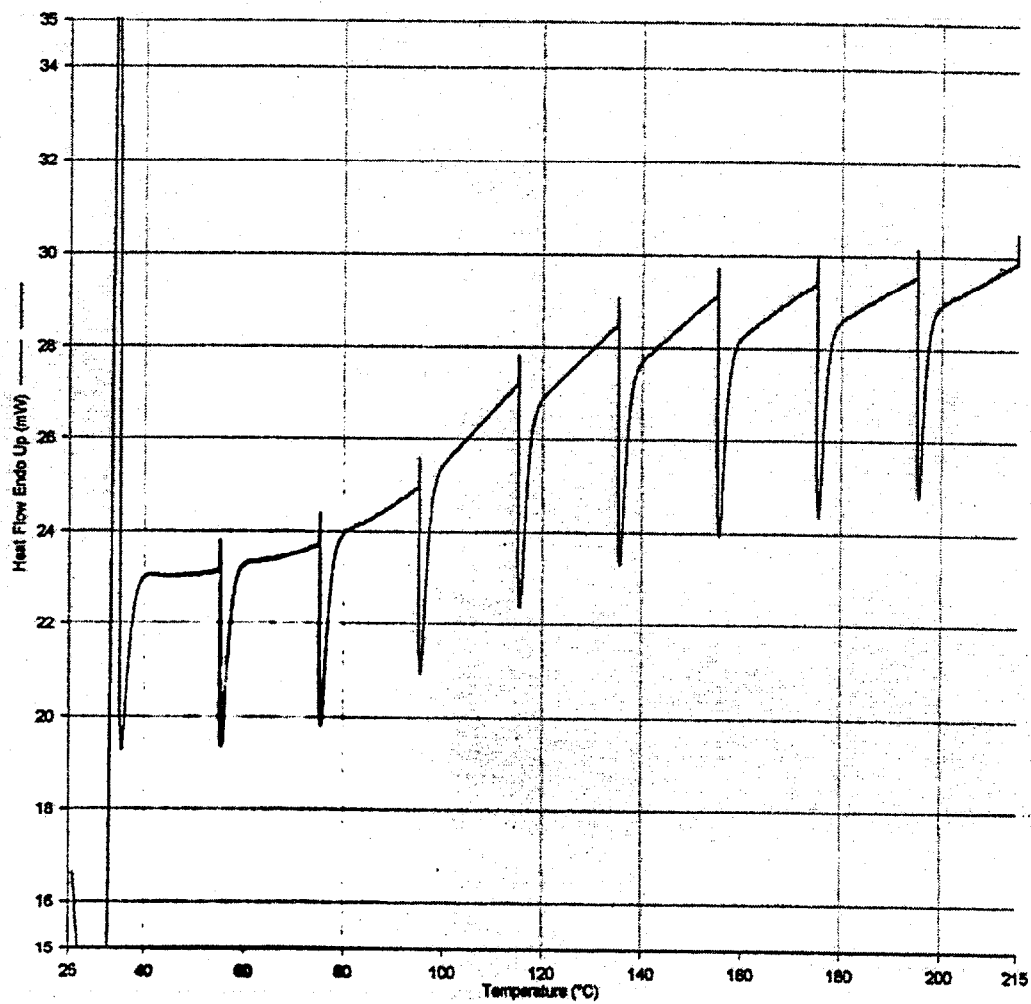


Fig. 4. DSC scan of pretreated Ionsiv® IE-911, lot 0999098810005.

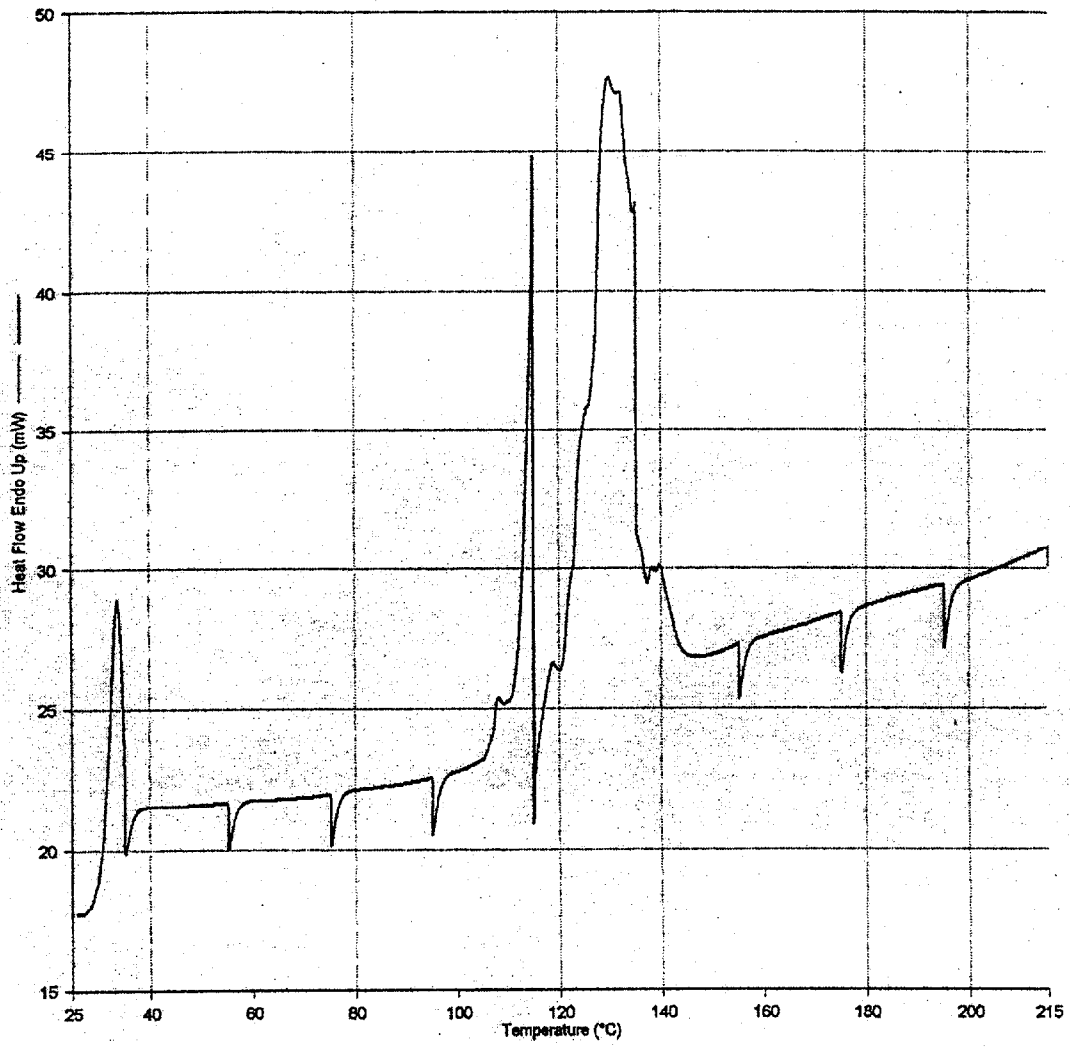


Fig. 5. DSC scan of precursor to CST binder.

Trade Secret 1 (TS1), a second laboratory chemical representing the binder in Ionsiv<sup>®</sup> IE-911, was also studied in the DSC (Fig. 6). It showed no reaction (endothermic or exothermic) peaks. Like the pretreated samples discussed above, the heat capacity of TS1 can be represented by two equations linear in temperature. Whereas the equations intersected at 130°C for the pretreated samples, the corresponding temperature for TS1 was closer to 100°C. No registered heat was associated with the change in temperature dependence of sample heat capacity in the region of 100°C. The TS1 samples showed neither graying nor charring during the heating in the DSC.

#### 4. THERMOPHYSICAL PROPERTIES OF SRS WASTE SIMULANTS

##### 4.1 PREPARATION OF WASTE SIMULANTS

The simulants were prepared using the method described by D. D. Walker in *Preparation of Simulated Waste Solutions*, WSRC-TR-99-00116, (April 15) 1999.<sup>1</sup> The densities of these simulants, as determined by final solution weight prior to filtration, were within 1% of theoretical values stated by Walker<sup>1</sup> for unfiltered preparations.<sup>3</sup> The consistent negative variance seen in Table 7 probably reflects a solution temperature higher than 22°C.

Table 7. Densities of SRS simulants determined on a weight basis

SRS simulant	Theoretical density (g/mL) <sup>a</sup>	Experimental density (g/mL)
Average	1.258	1.252
High OH <sup>-</sup>	1.244	1.230
High NO <sub>3</sub> <sup>-</sup>	1.271	1.264

<sup>a</sup>Solution temperature of 22°C.

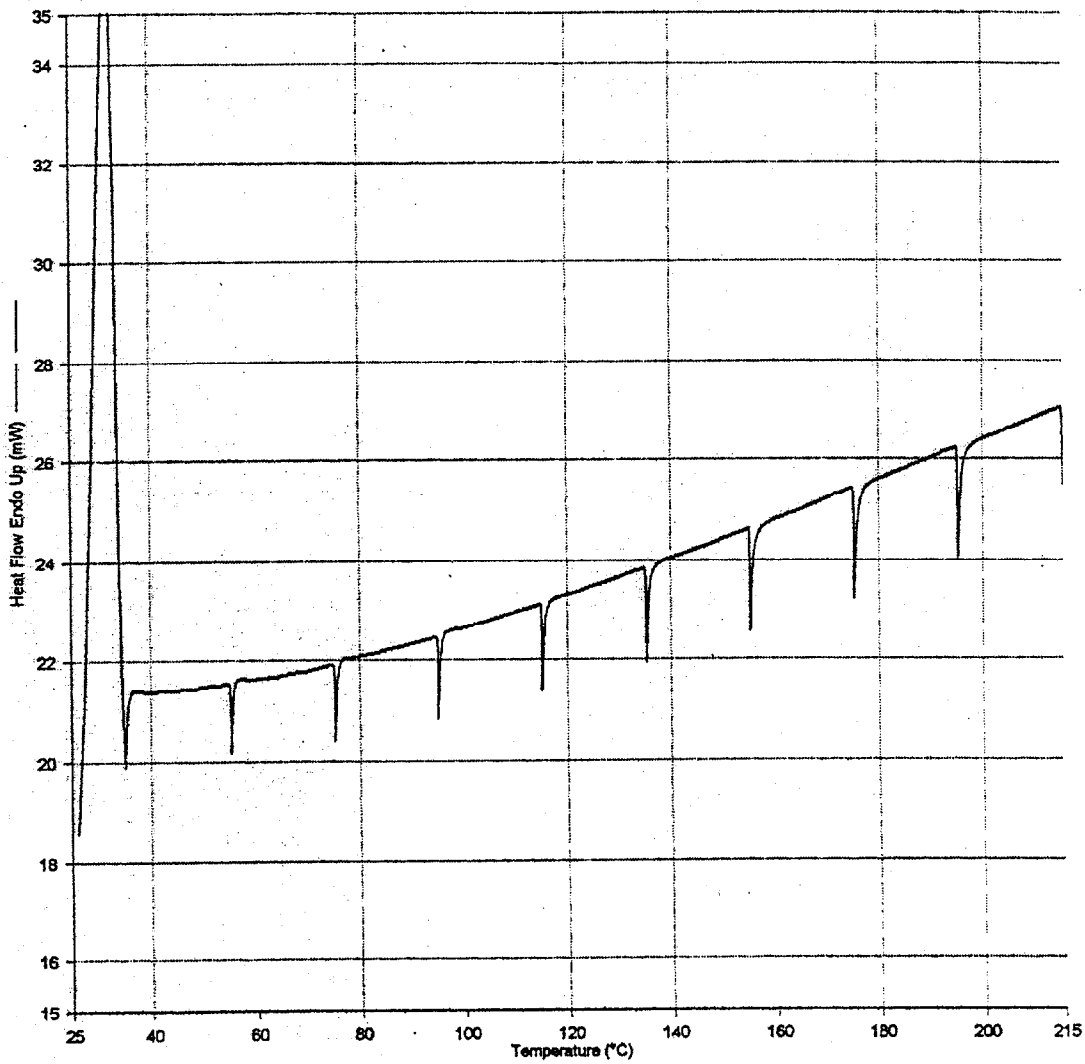


Fig. 6. DSC scan of CST binder in Ionsiv® IE-911.

## 4.2 DETERMINATION OF SOLUTION DENSITY

The densities of filtered Average, High OH<sup>-</sup>, and High NO<sub>3</sub><sup>-</sup> simulants were determined using an Anton Paar DMA 55 density meter in conjunction with a thermostated recirculating water cooler. The density cell was equipped with an iron-constantan thermocouple to determine solution temperature to within one-hundredth of a degree centigrade. Operation of the density meter was limited to 20–30°C due to water condensation on the surface of the density cell outside this range. Addition of a dry nitrogen purge gas to the instrument compartment would eliminate this problem in the future.

Sodium chloride standards and carbon dioxide-free water were used to calibrate the meter and verify the accuracy of the density measurements. Densities of the saline standards agreed with literature values to within 0.04 % (Fig. 7). The density of each of the simulants decreased linearly with temperature (Fig. 8). As can be seen from the regression equations in Table 8, the densities of all simulants were equally affected by temperature, within experimental error.

**Table 8. Regression equations for the determination of SRS simulant densities**

SRS simulant	Regression equation
Average	$1.2727 (\pm 0.0014) - 6.93e-04 (\pm 6.0e-05) \times \text{Temperature } (^{\circ}\text{C})$
High OH <sup>-</sup>	$1.2505 (\pm 0.0010) - 6.86e-04 (\pm 4.1e-05) \times \text{Temperature } (^{\circ}\text{C})$
High NO <sub>3</sub> <sup>-</sup>	$1.2840 (\pm 0.0011) - 7.15e-04 (\pm 4.8e-05) \times \text{Temperature } (^{\circ}\text{C})$

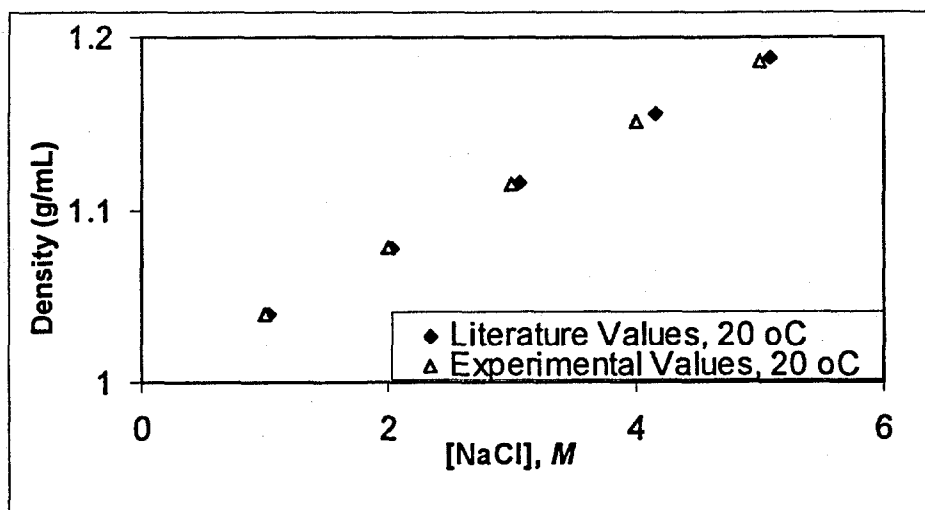


Fig. 7. Experimental versus literature values for densities of NaCl standards.

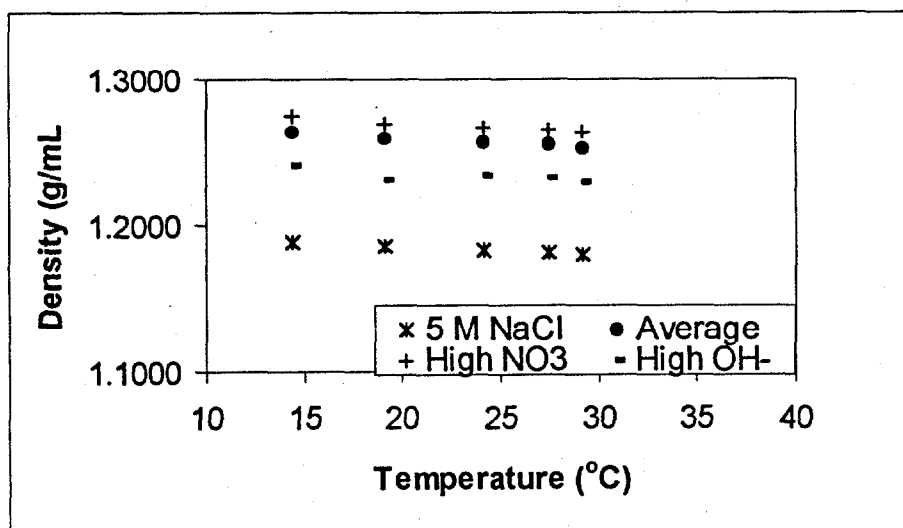


Fig. 8. Variation of simulant density with temperature.

The regression equations were used to calculate the densities of the simulants for the temperatures of interest, 10 and 30°C (see Table 9).

**Table 9 . Calculated densities for SRS simulants**

SRS simulant	Density (g/mL)	
	10°C	30°C
Average	1.2658	1.2519
High OH <sup>-</sup>	1.2433	1.2296
High NO <sub>3</sub> <sup>-</sup>	1.2768	1.2625

#### **4.3 FORMATION OF SOLIDS AT LOW TEMPERATURE**

The temperature at which solids are formed in the chilled simulants was determined by placing approximately 50 mL of each simulant in a chilled water/antifreeze bath. A glass-jacketed thermocouple was included to define actual solution temperature. The point of crystallization was determined in each case under the conditions of two scenarios: (1) a sample stirred intermittently as the temperature was reduced by 1°C every 1 to 2 h; and (2) a static sample remaining in the bath at a set temperature overnight. No formation of solids was observed with intermittent stirring in any simulant sample at temperatures equal to or greater than -4°C. Ice crystals were observed in the Average and High Nitrate simulants in static samples at -3 to -4°C. Both white amorphous solids and ice crystals were noted in the High Hydroxide simulant at these temperatures. All solids redissolved once the samples were brought to room temperature.

#### 4.4 DETERMINATION OF SIMULANT VISCOSITY

Viscosity determinations were performed using a Brookfield DV-III rheometer, a Brookfield UL adapter, a Haake A 81 circulator, a jacketed beaker, and an RTD temperature probe. The adapter, circulator, and beaker were connected with flexible tubing. The temperature probe and water were placed into the beaker. For each test condition, 16 mL of sample was transferred into the adapter, which was then attached to the rheometer. The circulator was set to the desired temperature for the viscosity measurement. The temperatures in the beaker and in the adapter were assumed to be equivalent. After a given sample had reached the desired temperature, it was allowed to equilibrate for 30 min and its viscosity was measured at 40, 50, 60, and 70 rpm. The corresponding shear rates were 49, 61, 73, and 86 s<sup>-1</sup>. At each rpm increment, measurements were taken every 10 s for a period of 2 min; this procedure was repeated to confirm the consistency of the results. The average viscosity at each rpm was then determined in each case. The individual viscosities were subsequently averaged to determine the final viscosity value for the specific test condition. The maximum experimental error was +/- 0.1 cP. Data were validated by also determining the viscosity of distilled, deionized water and comparing experimental with literature values. The results are included in Table 10:

Table 10. Viscosities of SRS simulants

Sample	Viscosity (cP)		
	10°C	20°C	30°C
Water (experimental)	1.34	1.06	0.84
Water (literature) <sup>a</sup>	1.31	1.00	0.80
Average SRS simulant	4.62	3.36	2.54
High OH <sup>-</sup> SRS simulant	4.81	3.57	2.56
High NO <sub>3</sub> <sup>-</sup> SRS simulant	3.97	3.13	2.40

<sup>a</sup>*International Critical Tables of Numerical Data, Physics, Chemistry, and Technology*, Vol. V, McGraw-Hill, Inc., New York, 1929, p. 15.

The High Hydroxide simulant had the highest viscosity of the three waste matrices at low temperature. However, the viscosities of all the simulants were essentially equivalent at elevated temperature. The SRS simulants were slightly shear thickening, or dilatant; an increase of 0.1 cP in the viscosity was noted when the shear rate was doubled. No hysteresis effect was observed when viscosity data were determined by “ramping” the shear rate either up or down during the determination.

#### 4.5 DETERMINATION OF HEAT CAPACITY

The determination of heat capacities of liquids using a DSC has been detailed in the literature numerous times. The method used in these measurements was the heat-equilibration-heat step method of Mraw and Naas.<sup>2</sup> The samples were confined in the same high-pressure cells used for DSC scans of solid CST. In the present study, each sample was sealed in the 50  $\mu$ L cells under air at ambient atmospheric pressure. Measurement of the simulant solutions was made in increments of 10 at a heating rate of 5 K/min with a 1-min equilibration interval between successive heats. The calibrant was sapphire [NIST Reference Standard Material (SRM 720)]; published heat capacity and enthalpy values were used.<sup>4</sup> The temperature scale of the DSC was calibrated before the measurements were made by determination of the melting point of NIST Standard Reference Material indium. Table 11 lists the results of the measurements made for each simulants.

Table 11. Determination of heat capacities for SRS simulants

Sample	Heat capacity ( $J \cdot g^{-1} \cdot ^\circ C$ )				
Water (experimental)	4.16	4.16	4.16	4.16	4.16
Water (literature)	4.182	4.179	4.179	4.181	4.184
Average SRS simulant	3.61	3.73	3.70	3.61	3.52
High OH <sup>-</sup> SRS simulant	3.43	3.47	3.45	3.43	3.44
High NO <sub>3</sub> <sup>-</sup> SRS simulant	3.35	3.37	3.39	3.40	3.41

#### 4.6 DETERMINATION OF THERMAL CONDUCTIVITY

The thermal conductivity of each waste simulant was determined using a Hot Disk Thermal Constants analyzer, based on the transient plane source method. A Kapton polyimide sensor was placed in an approximately 200-mL sample; three measurements were made for each simulant, with a 30- to 60- min relaxation time between each test. Each measurement represented the average of 5–7 calculations from the temperature-versus-time curve. To eliminate error due to thermal convection within the liquid samples, all data were taken within 5 s, and the first 2–3 s was used for the calculation of conductivity. All simulants, a 2.143 *m* NaCl standard, and deionized water had conductivities in the range of 0.6–0.7 W/m · K at 19 C. (Table 12). Experimental data indicate that there is no significant difference between the values for the simulants and that for the saline standard. However, the conductivity for water is several standard deviations lower than the remaining tabulated values. Literature values for the thermal conductivity of water and the saline standard at 20°C are 0.59 and 0.58, respectively<sup>12,13</sup>. The disparity in experimental values prompted the calculation of simulant conductivity derived from the composition of the individual simulants, based on the following algorithm<sup>14</sup>:

Table 12. Results of experimental thermal conductivity (W/m · K) measurements for SRS simulants

	Dionized		SRS simulant		
	water	2.142 <i>m</i> NaCl	Average	High OH <sup>-</sup>	High NO <sub>3</sub> <sup>-</sup>
Test 1	0.60	0.71	0.68	0.70	0.67
Test 2	0.61	0.73	0.68	0.68	0.66
Test 3	0.61	0.72	0.68	0.70	0.68
Average conductivity	0.61	0.72	0.68	0.70	0.67
Std. Dev.	0.01	0.01	0.00	0.01	0.01

$$\lambda_{\text{mix}}^{20^{\circ}\text{C}} = \lambda_{\text{H}_2\text{O}}^{20^{\circ}\text{C}} + \sum_i \sigma_i C_i, \quad (4)$$

where

$\lambda_{\text{mix}}^{20^{\circ}\text{C}}$  = thermal conductivity of the ionic solution at 20°C, W/m · K,

$\lambda_{\text{H}_2\text{O}}^{20^{\circ}\text{C}}$  = thermal conductivity of water at 20°C, W/m · K,

$C_i$  = concentration of electrolyte, g · mole/L, and

$\sigma_i$  = coefficient characteristic of each ion.

The thermal conductivity can be calculated for any temperature using the equation:

$$\lambda_{\text{mix}}(T) = \lambda_{\text{mix}}^{20^{\circ}\text{C}} \times \frac{\lambda_{\text{H}_2\text{O}}^T}{\lambda_{\text{H}_2\text{O}}^{20^{\circ}\text{C}}} \quad (5)$$

Calculated values in Table 13 show that the thermal conductivities for the simulants are the same as the thermal conductivity value for water and saline standards at a given temperature. Additionally, the conductivities of the liquids increase by approximately 3% for each increase in 10°C solution temperature.

Table 13. Calculated thermal conductivity values for SRS simulants

Anion	$\sigma_I$ coefficient <sup>a</sup>	NaCl	Simulant concentration (M)		
		standard (2.412 m)	Average	High OH <sup>-</sup>	High NO <sub>3</sub> <sup>-</sup>
OH <sup>-</sup>	2.09E-04		1.91	3.05	1.17
NO <sub>3</sub> <sup>-</sup>	-6.99E-05		2.14	1.08	2.84
NO <sub>2</sub> <sup>-</sup>	-4.65E-05		0.52	0.74	0.37
Cl <sup>-</sup>	-5.47E-05	2.142	0.02514	0.01037	0.04014
CO <sub>2</sub> <sup>-</sup>	-7.56E-05		0.16	0.17	0.16
PO <sub>4</sub> <sup>3-</sup>	-2.09E-04		0.01	0.008	0.01
C <sub>2</sub> O <sub>4</sub> <sup>2-</sup>	-3.49E-05		0.008	0.008	0.008
F <sup>-</sup>	2.09E-05		0.032	0.01	0.05
SiO <sub>4</sub> <sup>2-</sup>	-9.30E-05		0.004	0.004	0.004
MoO <sub>4</sub> <sup>2-</sup>			0.0002	0.0002	0.0002
AlO <sub>2</sub> <sup>-b</sup>	1.16E-05		0.31	0.27	0.32
SO <sub>4</sub> <sup>2-</sup>	1.16E-05		0.15	0.03	0.22
<b>Cation</b>					
Na <sup>+</sup>	0	2.142	5.6	5.6	5.6
K <sup>+</sup>	-7.56E-05		0.015	0.03	0.0041
H <sup>+</sup>	-9.07E-05		5.24E-14	3.28E-14	8.55E-14
Cs <sup>+</sup>	-1.16E-04		0.00014	0.00037	0.00014
<b>Calculated Thermal Conductivity <math>\lambda</math> (W/m · K)</b>					
$\lambda$ 10°C		0.5739	0.5742	0.5745	0.5740
$\lambda$ 20°C		0.5919	0.5922	0.5925	0.5920
$\lambda$ 30°C		0.6089	0.6092	0.6095	0.6090

<sup>a</sup>R. C. Reid, et al., *The Properties of Gases and Liquids*, 4th ed., McGraw-Hill, New York, 1987, p. 587.

<sup>b</sup>Assume that the aluminate coefficient is equivalent to that of sulfate.

## 5. SUMMARY

The physical properties of Ionsiv® IE-911 produced in 1998 by UOP were characterized by determining the size distribution, surface moisture content, sorbent porosity, and BET surface area of lot 999098810005.

Data were obtained for both as-received CST and pretreated (alkaline washed) Ionsiv® IE-911. Over 95 wt % of the CST was in the 30–50 mesh range (<-590/>-250  $\mu\text{m}$ ); less than 1% fines were present.

The average particle size for dry as-received and pretreated CST was  $410 \pm 10 \mu\text{m}$ . A comparison of dry-versus wet-sieve results indicates that the sorbent particle swells by approximately 9%; the pretreated material has a slightly higher value. The moisture content for each form of CST is ~7%. Sorbent porosity and surface area determinations, based on nitrogen adsorption, indicate that the BET surface area and pore volume values were higher in the as-received Ionsiv® IE-911,  $50 \text{ m}^2/\text{g}$ , and  $0.063 \text{ cm}^3/\text{g}$ , respectively.

Pretreated CST values were reduced by 30% in comparison. Each form of CST exhibited a Type II isotherm indicative of nonporous or macroporous adsorption. The hysteresis in the profile is that of Type H3, which is observed in sorbents composed of aggregates of plate-like particles similar to the layered crystalline structure of CST.

Solid-phase transitions in Ionsiv® IE-911 samples and pure CST powder without binder were determined using DSC data. The heat capacity of CST powder (Ionsiv® IE-910) varied linearly with temperature from 35 to 215°C, indicating that pure CST is stable over this temperature range. No signs of charring or color change were observed in the final heated sample. Studies of as-received Ionsiv® IE-911 samples (lots 999096810001 and 99909681004) prepared in early production runs show the presence of small exothermic heats at 145°C superimposed on the heat capacity-versus-temperature profile. Results obtained from more recently produced Ionsiv® IE-911 (lots 999098810005 and 999098810008) indicate that an endothermic reaction occurred throughout the temperature region 105–185°C. Additionally, a char residue

and “graying” of the CST particles were observed in the final heated sample. In comparison, DSC profiles of pretreated CST pellets did not exhibit an endothermic reaction and the heated sample was not discolored or charred. DSC scans of binder precursor in Ionsiv® IE-911 and the binder itself suggest that the endothermic reactions observed in the most recent production runs of the sorbent were probably due to the presence of binder precursor. The pretreatment of Ionsiv® IE-911 with sodium hydroxide appeared to wash the precursor contaminant from the sorbent pellets. Thus, stated equations derived for the determination of heat capacity for Ionsiv® IE-910 powder and Ionsiv® IE-911 pellets can be used provided that UOP does not change the formulation of the products and that there is no residual precursor to binder remaining in the final engineered CST.

Several thermophysical properties were determined for the three SRS simulants: Average, High OH<sup>-</sup> and High NO<sub>3</sub><sup>-</sup>. Of the parameters studied, the High NO<sub>3</sub><sup>-</sup> simulant had the greatest solution density at a given temperature, followed by the Average simulant. The density of each simulant decreased linearly over the 15–30°C range. All simulants were equivalently affected by temperature; a reduction of 10°C in solution temperature decreased the density by 0.5 %. When the solution temperature was decreased below -3°C, ice crystals formed in stagnant simulants. White amorphous solids began to form at -4°C only in unstirred High OH<sup>-</sup> simulant. All solids redissolved when they were brought to room temperature. The High OH<sup>-</sup> simulant had the greatest viscosity below room temperature. The viscosities of the simulants were essentially equivalent at 30°C (2.5 cP). The heat capacities of the simulants ranged from 3.35 to 3.70 J·g<sup>-1</sup>·°C for the 20–60°C temperature range. The Average simulant consistently had the greatest heat capacity of the three waste matrices. There appeared to be no significant difference in the thermal conductivities of the simulants; 0.7 W/m·K was a typical value. Calculated data suggest that the thermal conductivity increased by 3% for every 10°C increase in solution temperature.

This compilation of thermophysical data should help to resolve questions associated with the use of Ionsiv<sup>®</sup> IE-911 to decontaminate SRS waste streams. The research conducted thus far with filtered SRS waste simulants suggests that potential solids formation associated with the cooling of feed streams should be minimal. Heat capacity data that will aid in calculating a total heat balance for large-scale CST columns are also provided. Finally, the source of an endothermic reaction in as-received Ionsiv<sup>®</sup> IE-911 appears to be the presence of small amounts of binder precursor that can be removed using an alkaline pretreatment of the CST.

## 6. REFERENCES

1. P. L. Rutland, "Thermal and Hydraulic Property Determination," HLW-SDT-TTR -99-10.0 (Jan. 25, 1999).
2. W. V. Steele, "Technical Task Plan for Thermal & Hydraulic Property Determinations," ORNL/CF-99/4.
3. D. D. Walker, *Preparation of Simulated Waste Solutions*, WSRC-TR-99-00116, April 15, 1999.
4. D. T. Bostick, S. M. DePaoli, and B. Guo, *Evaluation of Improved Techniques for the Removal of Fission Products from Process Wastewater and Groundwater: FY 1997 Status*, ORNL/TM-13497, Oak Ridge National Laboratory (Feb. 1998).
5. H. Lao and C. Detellier, "Microporosity" in *Comprehensive Supramolecular Chemistry*, Vol. 8, J. L. Atwood et al. (ed.), Elsevier Sci. Ltd., New York, 1996, p. 277-306.
6. R. Baum, *Cesium Cut from Radioactive Waste*, *C&E News*, July 13, 1992, 26.
7. R. G. Anthony, R. G. Dosch, Ding Gu, and C. V. Philip, *Use of Silicotitanates for Removing Cesium and Strontium from Defense Waste*, *Ind. Eng. Chem. Res.*, **33**, 2702-2705 (1994).
8. R. G. Dosch, N. E. Brown, H. P. Stephens and R. G. Anthony, *Treatment of Liquid Nuclear Wastes with Advanced Forms of Titanate Ion Exchangers*, '93 Waste Mgmt. Symp., Tucson, Ariz. (1993).
9. S. C. Mraw and D. F. Nass. "The Measurement of Accurate Heat Capacities of Differential Scanning Calorimetry. Comparison of d.s.c. results on Pyrite (100 to 800 K) with Literature Values from Precision Adiabatic Calorimetry." *J. Chem. Thermodynamics*. **11**, 567-584 (1979).

10. S. E. Knipmeyer, D. G. Archer, R. D. Chirico, B. E. Gammon, I. A. Hossenlopp, A. Nguyen, N. K. Smith, W. V. Steele, and M. M. Strube, "High-temperature Enthalpy and Critical Property Measurements Using a Differential Scanning Calorimeter," *Fluid Phase Equilibria* (1989), **52**, 185-192 (1989).
11. D. A. Ditmars, S. Ishihara, S. S. Chang, G. Bernstein, and E. D. West, "Enthalpy and Heat-Capacity Standard Reference Material Synthetic Sapphire ( $\alpha\text{-Al}_2\text{O}_3$ ) from 10 to 2250 K," *J. Res. Nat. Bur. Stand.* **87**, 159-163 (1982).
12. *CRC Handbook of Chemistry and Physics*, 61st ed, R. C. Weast (ed.), Boca Raton, Fla., 1980, p. E-11.
13. *International Critical Tables of Numerical Data, Physics, Chemistry, and Technology*, Vol. V, McGraw-Hill, Inc., New York, 1929, p. 229).
14. R. C. Reid, J. M. Prausnitz, B. E. Poling, *The Properties of Gases and Liquids*, 4th ed., McGraw-Hill, New York, 1987, p. 587.

**INTERNAL DISTRIBUTION**

1. E. C. Beahm
- 2-11. D. A. Bostick
12. J. L. Collins
13. R T. Jubin
14. D. D. Lee
15. C. P. McGinnis
16. S. M. Robinson
17. W. V. Steele
18. P. A. Taylor
19. T. D. Welch

**EXTERNAL DISTRIBUTION**

- 20-27. Tanks Focus Area Technical Team  
B. J. Williams, Pacific Northwest National Laboratory, P.O. Box 999, MSIN K9-69, Richland, WA 99352
28. Tanks Focus Area Field Lead  
T. P. Pietrok, U.S. Department of Energy, Richland Operations Office, P.O. Box 550, MSK8-50, Richland, WA 99352
29. Oak Ridge Reservation  
J. R. Noble-Dial, U.S. Department of Energy, Oak Ridge Operations Office, P.O. Box 2001, Oak Ridge, TN 37830-8620
30. Savannah River Site  
Jeff Barnes, Westinghouse Savannah River Company, P.O. Box 616, 704-3N, Aiken, SC 29808
31. Mark Barnes, Westinghouse Savannah River Company, P.O. Box 616, 773-A, Aiken, SC 29808
32. Joe Carter, Westinghouse Savannah River Company, P.O. Box 616, 704-3N, Aiken, SC 29808
33. Connie Dyer, Westinghouse Savannah River Company, P.O. Box 616, 704-3N, Aiken, SC 29808
34. Hank Elder, Westinghouse Savannah River Company, P.O. Box 616, 704-3N, Aiken, SC 29808
35. Sam Fink, Westinghouse Savannah River Company, P.O. Box 616, 773-A, Aiken, SC 29808
36. T. S. Gutmann, U.S. Department of Energy, Savannah River Operations Office, P.O. Box A, Aiken, SC 29802
37. David Hobbs, Westinghouse Savannah River Company, P.O. Box 616, 773-A, Aiken, SC 29808

38. Roy Jacobs, Westinghouse Savannah River Company, P.O. Box 616, 704-3N, Aiken, SC 29808
39. Jim McCullough, Westinghouse Savannah River Company, P.O. Box 616, 704-3N, Aiken, SC 29808
40. J. P. Morin, Westinghouse Savannah River Company, Savannah River Technology Center, 703-H Bldg., Aiken, SC 29808
41. Donie Nichols, Westinghouse Savannah River Company, P.O. Box 616, 773-55A, Aiken, SC 29802
42. Lou Papouchado, Westinghouse Savannah River Company, P.O. Box 616, 773-A, Aiken, SC 29808
43. Reid Peterson, Westinghouse Savannah River Company, P.O. Box 616, 773-A, Aiken, SC 29808
44. Steve Piccolo, Westinghouse Savannah River Company, P.O. Box 616, 704-3N, Aiken, SC 29808
45. Michael Poirier, Westinghouse Savannah River Company, P.O. Box 616, 679-T, Aiken, SC 29808
46. Ken Rueter, Westinghouse Savannah River Company, P.O. Box 616, 704-3N, Aiken, SC 29808
47. Bill Spader, U.S. Department of Energy, Westinghouse Savannah River Company, P.O. Box 616, 704-S, Aiken, SC 29808
48. Pat Suggs, Westinghouse Savannah River Company, P.O. Box 616, 704-3N, Aiken, SC 29808
49. Walt Tamosaitis, Westinghouse Savannah River Company, P.O. Box 616, 773-A, Aiken, SC 29808
50. Bill Van Pelt, Westinghouse Savannah River Company, P.O. Box 616, 773-43A, Aiken, SC 29808
51. D. D. Walker, Westinghouse Savannah River Company, P.O. Box 616, 773-A, Aiken, SC 29808